

# Complexity in charge transport for multiwalled carbon nanotube and poly(methyl methacrylate) composites

Heon Mo Kim, Mahn-Soo Choi, and Jinsoo Joo\*

*Department of Physics and Institute for Nano Science, Korea University, Seoul 136-713, Korea*

Sin Je Cho

*Ijin Nanotech Co., Ltd., Kangseo-Ku, Seoul 157-810, Korea*

Ho Sang Yoon

*NOVATEMS Inc., DangJeong-Dong, Gunpo-City, Kyunggi-Do 435-831, Korea*

(Received 10 April 2006; revised manuscript received 22 June 2006; published 3 August 2006)

We report on studies of the charge transport mechanism of the composites of multiwalled carbon nanotubes (MWCNTs) and poly (methyl methacrylate) (PMMA). The MWCNTs were synthesized by a chemical vapor deposition method using Fe as a catalyst. The dc conductivity ( $\sigma_{dc}$ ) and its temperature dependence [ $\sigma_{dc}(T)$ ] were measured in a temperature range of 0.5–300 K to study the charge transport mechanism of the composites. The  $\sigma_{dc}$  of composites at room temperature increased as the MWCNT concentration increased, which shows typical percolation behavior with percolation threshold of  $p_c$  at  $\sim 0.4$  wt % of the MWCNTs. The  $\sigma_{dc}(T)$  of the MWCNT-PMMA composites were fitted to the combination of Sheng's fluctuation induced tunneling (FIT) model and the one-dimensional variable range hopping (1D VRH) model. The tunneling mechanism and the 1D VRH transport were attributed to the charge tunneling between MWCNT clusters and the charge hopping through 1D MWCNTs, respectively. Magnetoresistance (MR) of MWCNT-PMMA composites was measured up to 9 T of magnetic field. The results of MR and  $\sigma_{dc}(T)$  showed that the FIT model was dominant in the low temperature region ( $T \lesssim 10$  K), while the 1D VRH process became dominant as the temperature increased ( $10 \text{ K} \lesssim T \lesssim 300$  K). We observed unusually large negative MR in the composites at the lower temperatures ( $T < 4$  K) due to FIT conduction. We related the parameters specifying charge transport to the percolation structures of MWCNT-PMMA composites based on the results of temperature dependence of  $\sigma_{dc}$  and of the MR.

DOI: [10.1103/PhysRevB.74.054202](https://doi.org/10.1103/PhysRevB.74.054202)

PACS number(s): 73.63.Fg, 72.15.Cz, 71.20.Lp, 73.43.Qt

## I. INTRODUCTION

Research on carbon nanotubes has rapidly increased during this last decade. Single-walled carbon nanotubes (SWCNTs) have been studied in the academic field because of their low dimensional nature with well-defined structure.<sup>1</sup> Multiwalled carbon nanotubes (MWCNTs) have been regarded as excellent nanomaterials for fundamental research as well as industrial applications.<sup>2,3</sup> Research is important not only for the application of MWCNTs and not only for understanding intrinsic properties of MWCNTs, but also for low cost mass production of these MWCNTs. The composites of MWCNTs with conventional polymers have been emphasized for commercial applications. In these applications, the electrical and thermal properties of the MWCNTs should be optimized with flexibility and an easy mixing process obtained from the polymers. To optimize the electrical properties in the composites, it is required to study the charge transport mechanism for the various composites of the MWCNTs with insulating polymers.<sup>4,5</sup> Such studies include the temperature dependence of electrical conductivity and of magnetoresistance (MR).

The electrical conduction in the composites of conducting MWCNTs and insulating poly (methyl methacrylate) (PMMA) have been known as percolating behavior. The studies of MWCNT composites with poly (*m*-phenylenevinylene-*co*-2,5-dioctyloxy-*p*-phenylenevinylene)

or polyvinylalcohol showed that the charge transport mechanism was mainly affected by fluctuation induced tunneling (FIT). Here the dc conductivity ( $\sigma_{dc}$ ) at room temperature (RT) [ $\sigma_{dc}(\text{RT})$ ] and the ac conductivity ( $\sigma_{ac}$ ) as a function of MWCNT concentration had been measured for the analysis.<sup>5</sup> Sheng's FIT model<sup>6</sup> has been in competition with the variable range hopping (VRH) model<sup>7</sup> in explaining the charge transport mechanism in the composites of MWCNTs and PMMA. In order to clarify the charge transport mechanism of the MWCNT-polymer composites, experiments addressing the temperature dependence of  $\sigma_{dc}$  [ $\sigma_{dc}(T)$ ] and the MR in the lower temperature region ( $T \lesssim 4$  K) should be performed and results then analyzed.

In this study, we synthesized composites of MWCNTs and PMMA in the form of free-standing films. The percolation behavior as a function of the mass fraction of the MWCNTs in the PMMA background was observed from the measured  $\sigma_{dc}(\text{RT})$ . From  $\sigma_{dc}(T)$  in the temperature range from 0.5 to 300 K, the combination of Sheng's FIT model and the one-dimensional (1D) VRH model was suggested for explaining the charge transport mechanism of the systems. The results of temperature and magnetic field dependence of the MR of the systems supported the complexity of charge transport using the combination of the FIT and 1D VRH models.

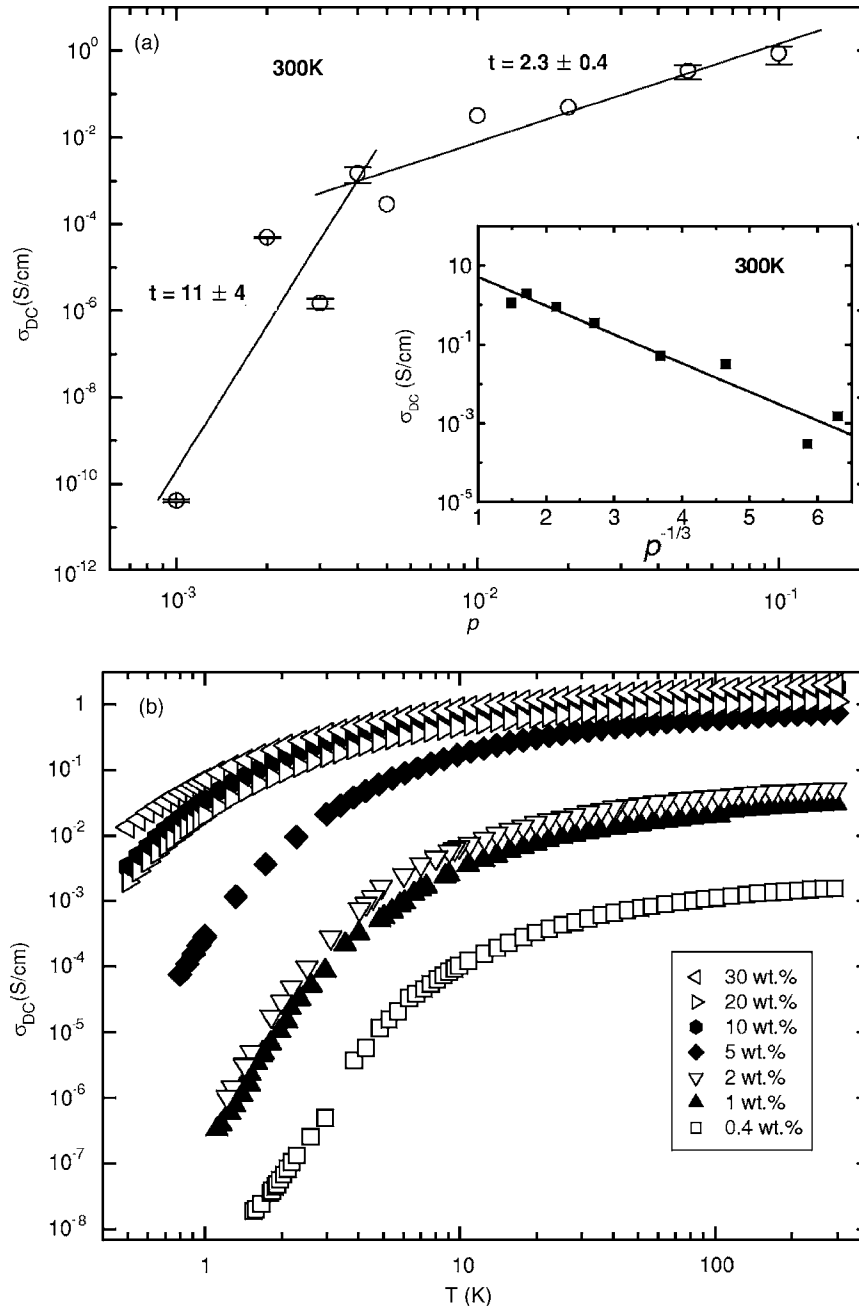


FIG. 1. (a) dc conductivity at room temperature [ $\sigma_{dc}(\text{RT})$ ] of MWCNT-PMMA composites as a function of the MWCNT mass concentrations ( $p$ ). Inset: Plot of  $\sigma_{dc}(\text{RT})$  as a function of  $p^{-1/3}$ . (b) Temperature dependence of dc conductivity [ $\sigma_{dc}(T)$ ] of MWCNT-PMMA composites.

## II. EXPERIMENT

The MWCNTs were synthesized by the chemical vapor deposition method using Fe as the catalyst, which were provided by Iljin Nanotech Co., Ltd.<sup>8</sup> The MWCNTs were dispersed in toluene with PMMA through stirring and sonication for 24 h. The weight (wt)% of MWCNTs varied from 0.1 to 40 wt %. The dispersed solution was cast onto a teflon substrate and dried in a vacuum oven at 40 °C over 12 h to prepare free-standing films. The thickness of the free-standing films was from  $\sim 60$  to  $\sim 165$   $\mu\text{m}$ . The homogeneous dispersion of MWCNTs in the composites was confirmed by means of SEM, TEM, and XPS, which were reported earlier.<sup>3,9</sup>

For the measurement of  $\sigma_{dc}(T)$ , the 4-probe contact method was used to eliminate contact resistance. The mea-

surement for  $\sigma_{dc}(T)$  was in the temperature range from 0.5 to 300 K and was made by using the physical property measurement system (Quantum Design 6000 PPMS). Quantum design model 6000 9T PPMS was used for measuring the MR in the temperature range of 0.5 to 300 K with the magnetic field up to 9 T. The applied magnetic field for the MR measurements of the systems was perpendicular to the direction of the applied current in the 4-probe contact method.

## III. RESULTS AND DISCUSSION

Figure 1(a) shows  $\sigma_{dc}(\text{RT})$  as a function of the MWCNT mass concentrations ( $p$ ). The  $\sigma_{dc}(\text{RT})$  of the composites increased up to ten orders in magnitudes as the MWCNT con-

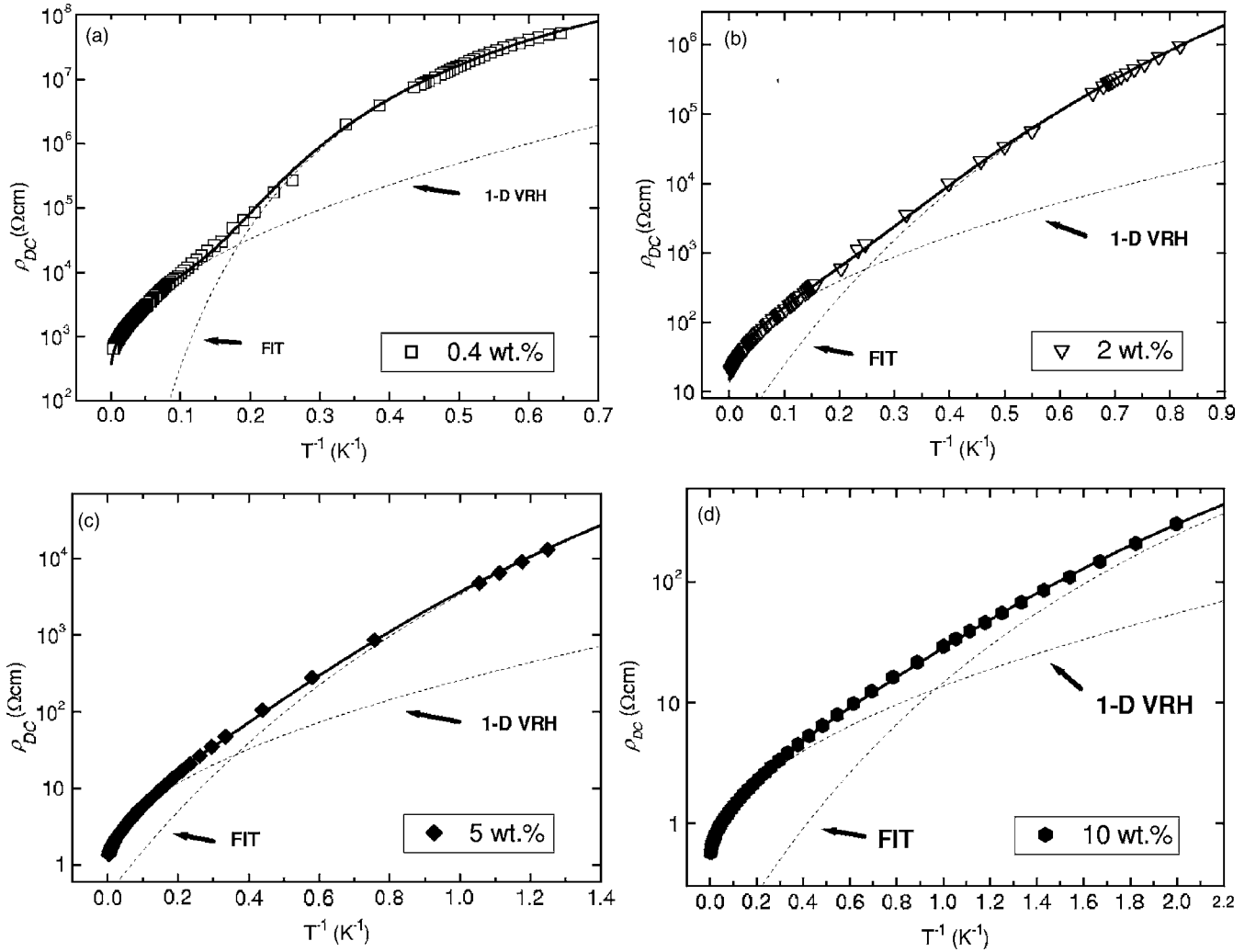


FIG. 2. Temperature dependence of resistivity of MWCNT-PMMA composites with (a) 0.4 wt %, (b) 2 wt %, (c) 5 wt %, and (d) 10 wt % of MWCNT concentration. The fitting lines were from the linear combination of the Sheng’s fluctuation induced tunneling (FIT) model and the one-dimensional variable range hopping (1D VRH) model.

centration increased up to 30 wt %. The plot of  $\sigma_{dc}(RT)$  vs  $p$  for the MWCNT-PMMA composites showed typical percolation behavior described as  $\sigma(p) \propto |p - p_c|^t$ . The critical exponent  $t$  in Fig. 1(a) varied from  $11 \pm 4$  to  $2.3 \pm 0.4$  at  $\sim 0.4$  wt % of MWCNT concentration. This implies that the percolation threshold was at a  $p_c \sim 0.004$ . The  $p_c$  was converted to the volume fraction as  $f_c \sim 0.0087$ . For conventional three-dimensional (3D) systems, the percolation threshold by volume fraction is 0.16.<sup>10</sup> The relatively small value of the percolation threshold in the MWCNT composites studied here was accounted for MWCNTs having one-dimensional (1D) shape with a large aspect ratio. The inset of Fig. 1(a) shows the plot of  $\sigma_{dc}(RT)$  vs  $p^{-1/3}$ , which followed the expected linear relation. Kilbride *et al.* reported the charge transport mechanism of the percolating system consisted of CNTs and insulating polymers. It was described by the FIT model,<sup>5</sup> where the relation between  $\sigma_{dc}$  and the MWCNT concentration ( $p$ ) was described as  $\ln \sigma_{dc} \propto -p^{-1/3}$ . However, the deviation from the fitting line at  $p < 0.004$  as shown in the inset of Fig. 1(a) implies that another charge transport process might be considered in the composites. Fig-

ure 1(b) shows  $\sigma_{dc}(T)$  in the MWCNT-PMMA composites above the percolation threshold ( $p_c = 0.004$ ). The  $\sigma_{dc}$  of all composites of MWCNT-PMMA decreased with decreasing temperature, implying charge localization. The ratios of  $\sigma_{dc}(RT)$  to  $\sigma_{dc}(T = 2.1 \text{ K})$  [ $\sigma_r \equiv \sigma_{dc}(RT) / \sigma_{dc}(T = 2.1 \text{ K})$ ]

TABLE I. Fitting parameters of  $T_1$ ,  $T_0$ , and  $T_{1D}$  for the MWCNT-PMMA composites based on the combination of the Sheng’s FIT and the 1D VRH models.

wt % of MWCNTs	$T_1$ (K)	$T_0$ (K)	$T_{1D}$ (K)
0.4	195.13	6.68	108.99
1	39.23	1.58	77.55
2	29.80	1.02	62.69
5	13.90	0.55	31.31
10	8.21	0.48	11.31
20	8.13	0.49	11.55
30	8.92	0.66	9.80

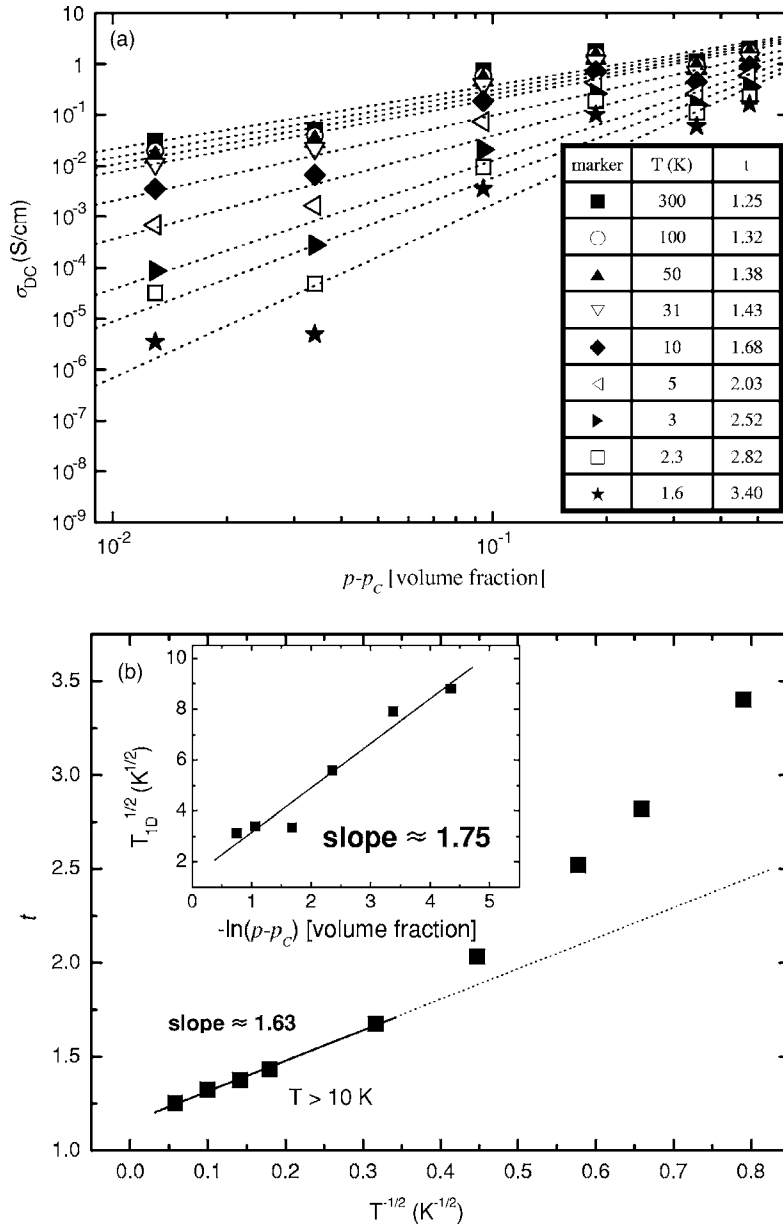


FIG. 3. (a) Variation of percolation exponent  $t$  at different temperatures. Inset table: Values of  $t$  at different temperatures. The dotted lines are a guide to the eye. (b) Temperature dependence of percolation critical exponent  $t$  above 10 K based on the 1D VRH model. Inset:  $T_{1D}^{1/2}$  vs  $-\ln(p-p_c)$ ; percolation behavior of activation energy ( $T_{1D}$ ) of the 1D VRH model.

were calculated. For the composites with MWCNT concentrations of 10–30 wt %, temperature dependences of  $\sigma_r$  were relatively weak as  $\sigma_r=8.40$ – $11.81$ . However, for the composites with MWCNT concentrations below 2 wt %,  $\sigma_r$  increased considerably up to  $\sim 1.9 \times 10^4$  as the MWCNT concentration decreased, indicating more insulating behavior.

Figures 2(a)–2(d) show plots of dc resistivity ( $\rho_{dc}$ ) vs  $T^{-1}$  for the composite films of 0.4, 2, 5, and 10 wt % of MWCNT concentration, respectively. We analyzed that it was impossible to fit the temperature dependence of resistivity [ $\rho_{dc}(T) \equiv \sigma_{dc}^{-1}(T)$ ] over the whole temperature region including the lower temperature range ( $0.5 \text{ K} \leq T \leq 300 \text{ K}$ ) just by using Sheng's FIT model. Because of the complexity of charge transport in MWCNT-PMMA composites, we used a linear combination of Sheng's FIT model and the 1D VRH model as follows:<sup>11,12</sup>

$$\sigma_{dc}(T) = \sigma_{1D} \exp\left[-\left(\frac{T_{1D}}{T}\right)^{1/2}\right] + \sigma_0 \exp\left(\frac{-T_1}{T+T_0}\right), \quad (1)$$

where the first and the second terms originated from the 1D VRH model and the Sheng's FIT model, respectively.<sup>6,7</sup> Here,  $\sigma_{1D}$  and  $\sigma_0$  are the proportionality constants,  $T_{1D}$  is the activation energy in the 1D VRH model,  $T_1$  is the temperature below which the conduction is dominated by the charge tunneling through the barrier, and  $T_0$  is the temperature above which the thermally activated conduction over the barrier begins to occur. The  $\rho_{dc}(T)$ 's of all composites of MWCNT-PMMA studied here were fitted to the Eq. (1), as shown in Fig. 2. From the results of  $\rho_{dc}(T)$  and the fitting curves based on Eq. (1), Sheng's FIT model was dominant for the charge transport mechanism in composites below 10 K, which can be attributed to tunneling conduction

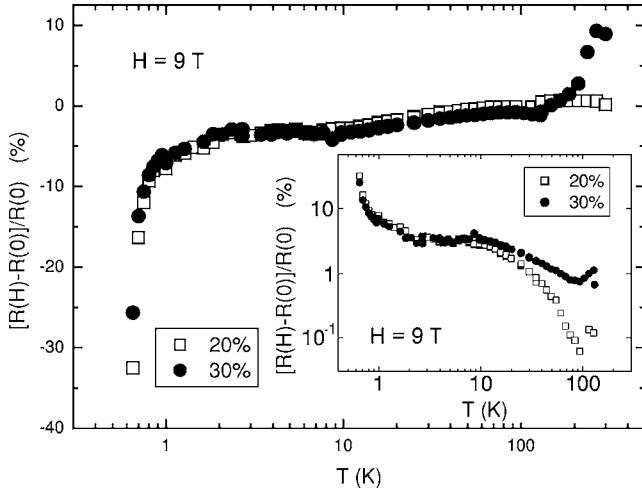


FIG. 4. Temperature dependence ( $0.7 \text{ K} \leq T \leq 300 \text{ K}$ ) of the MR of MWCNT-PMMA composites with 20 and 30 wt % of MWCNTs at 9 T of magnetic field. Inset: Temperature dependence of absolute value of MR in log scale.

through insulating PMMA barriers between MWCNT networks. As temperature increased above 10 K, the 1D VRH process between MWCNTs or MWCNT networks became dominant as shown in Figs. 2(a)–2(d). It is noted that the  $\rho_{dc}(T)$  of the composites with 20 and 30 wt % of MWCNTs was also fitted to Eq. (1). The values of  $T_1$ ,  $T_0$ , and  $T_{1D}$ , obtained from the fitting curves of the FIT and 1D VRH models are listed in Table I. The values of  $T_1$ ,  $T_0$ , and  $T_{1D}$  decreased with increasing concentration of MWCNTs, implying the lowering of activation energies.

Figure 3(a) shows the variation of percolation exponent  $t$  at different temperatures obtained from the results of  $\sigma_{dc}(T)$  and  $\sigma = \sigma'_0(p-p_c)^t$ . The percolation exponent  $t$  increased as temperature decreased as listed in the inset table of Fig. 3(a). Our analysis indicated that the percolation behavior of MWCNT-PMMA composites was affected by temperature due to the different activation energies. In general, the percolation exponent  $t$  increases as the dimensionality of the systems increases, and  $p_c$  of the system also depends on the dimensionality of the systems.<sup>10</sup> When the percolation relation  $\sigma = \sigma'_0(p-p_c)^t$  is combined with the first term of Eq. (1), i.e., the 1D VRH model, the relation between the  $t$  and temperature above 10 K can be described as in Eq. (2):

$$t = \frac{-1}{\ln(p-p_c)} \left( \frac{T_{1D}}{T} \right)^{1/2} + \frac{\ln(\sigma_{1D}/\sigma'_0)}{\ln(p-p_c)} \propto T^{-1/2}. \quad (2)$$

Figure 3(b) shows  $t$  vs  $T^{-1/2}$  based on Eq. (2). The values of  $t$  above 10 K were fitted to Eq. (2) with the slope of  $\sim 1.63$ . The activation energy  $T_{1D}$  was directly related to  $\ln(p-p_c)$  through the value of the slope. The inset of Fig. 3(b) shows  $T_{1D}^{1/2}$  as a function of  $-\ln(p-p_c)$ , using the  $T_{1D}$  values in Table I. The slope of the plot of  $T_{1D}^{1/2}$  vs  $-\ln(p-p_c)$  was  $\sim 1.75$ , which was similar to the value of the slope ( $\sim 1.63$ ) using Eq. (2). Therefore the activation energy in the 1D VRH model can be described as a function of the MWCNT concentration ( $p-p_c$ ),

$$T_{1D} \propto [\ln(p-p_c)]^2. \quad (3)$$

For  $n$ -dimensional conductors dominated by the VRH conduction, Eq. (3) can be generalized to be

$$T_{n-D} \propto [\ln(p-p_c)]^{n+1}. \quad (4)$$

Below 10 K, the charge transport in MWCNT-PMMA composites was dominated by the Sheng's FIT process. The percolation exponent  $t$  due to the tunneling conduction was related to the second fitting term of Eq. (1) with  $\sigma = \sigma'_0(p-p_c)^t$ . We, then, obtained the following relation:

$$t = \frac{-1}{\ln(p-p_c)} \left( \frac{T_1}{T} - \frac{T_0 T_1}{T^2} \right) + \frac{\ln(\sigma'_0/\sigma'_0)}{\ln(p-p_c)}. \quad (5)$$

This is not a simple equation to obtain the generalized relation of  $T_0$  and  $T_1$  with  $p-p_c$ .

Figure 4 presents temperature dependence of MR [MR( $T$ )] of MWCNT-PMMA composites with MWCNT concentrations of 20 and 30 wt % from 0.7 to 300 K. As the temperature decreased, the MR of MWCNT-PMMA composites negatively increased. The inset of Fig. 4 shows absolute

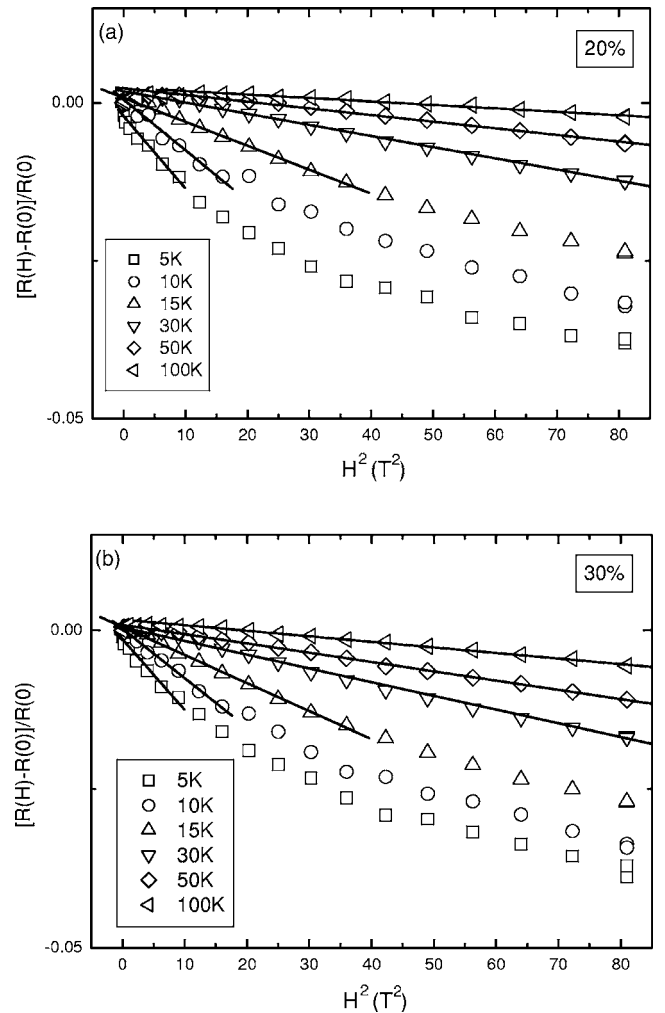


FIG. 5. (a) MR vs  $H^2$  at various temperatures for 20 wt % of MWCNT-PMMA composites. (b) MR vs  $H^2$  at various temperatures for 30 wt % of MWCNT-PMMA composites.

values of  $MR(T)$  of the systems on a log scale. From 300 K down to  $\sim 10$  K, we observed that the MR negatively increased by  $\sim 3\%$  compared to the zero field resistance [ $R(H=0)$ ]. As the temperature decreased from 10 to 0.7 K, the negative MR of the MWCNT-PMMA composites rapidly increased from  $\sim 2.8\%$  to  $\sim 32\%$  compared to  $R(H=0)$ , as shown in the inset of Fig. 4. This suggests that a different transport mechanism might be applied in the lower temperature range. The rapid change of the negative MR below  $\sim 10$  K qualitatively agrees with the results and analysis of  $\sigma_{dc}(T)$ .

The negative MR can be caused by the VRH process, FIT, or weak localization effect.<sup>12,13</sup> For the networks of SWCNTs or MWCNTs, the results of the MR have been explained by the VRH model<sup>12</sup> or the weak localization effect.<sup>13</sup> The negative MR in terms of the VRH model is related to the applied magnetic field ( $H$ ) and temperature described as

$$\frac{\sigma(H,T) - \sigma(0,T)}{\sigma(0,T)} \propto \frac{1}{2} \left( \frac{\beta n}{n+1} \right)^2 \left[ \frac{g\mu_B H}{2(E_C - E_F)} \right]^2 \left( \frac{T_0}{T} \right)^{2/(n+1)}, \quad (6)$$

where  $|\frac{1}{2}g\mu_B H / (E_C - E_F)| \ll 1$  is assumed, i.e., the weak magnetic field limit. Here,  $\beta$  is approximately 1,  $n$  is the dimensionality constant,  $g$  is the effective  $g$ -factor,  $\mu_B$  is the Bohr magneton, and  $E_C$  is the mobility edge.<sup>14</sup> Figures 5(a) and 5(b) show magnetic field dependence of the MR of MWCNT-PMMA composites, with 20 and 30 wt % of MWCNTs, respectively, at various temperatures ( $5 \text{ K} \leq T \leq 100 \text{ K}$ ). Based upon Eq. (6), it is expected that the MR would show the quadratic magnetic field dependence ( $\propto H^2$ ) in the weak field limit, which was determined from  $\frac{1}{2}k_B T \approx \mu_B H \leq |E_C - E_F|$ . With  $T \geq 30 \text{ K}$ , the MR of the composites with 20 and 30 wt % of MWCNTs followed the quadratic field dependence in the weak field limit, which supports the domination of the VRH model for the charge transport mechanism. As shown in Figs. 5(a) and 5(b), the MR in the

temperature range below 15 K did not follow the quadratic field dependence in the whole applied magnetic field. This might suggest that another transport model, such as the FIT model, can dominate the charge transport mechanism in lower temperature range. The results of the magnetic field dependence of the MR also supported the results and analysis of  $\sigma_{dc}$ .

#### IV. SUMMARY

We synthesized MWCNT-PMMA composites with various concentrations of MWCNTs. The measured  $\sigma_{dc}(RT)$  of the MWCNT-PMMA composites showed percolation behavior with relatively lower percolation threshold ( $p_c \sim 0.004$ ), which originated from the 1D shape of conducting MWCNTs and their network formation in the composites. The charge transport properties of the MWCNT-PMMA composites were explained in terms of a combination of the Sheng's FIT and the 1D VRH models. The relation between the parameters specifying charge transport and percolation behavior were described as  $T_{n-D} \propto [\ln(p-p_c)]^{n+1}$  for the  $n$ -dimensional VRH model. From the measurements of  $\rho_{dc}(T)$  and the MR, we observed that the 1D VRH conduction was dominant in charge transport at a relatively higher temperature ( $10 \text{ K} \leq T \leq 300 \text{ K}$ ) for the composites with higher concentrations of MWCNTs. The Sheng's FIT model was fitted to the results of  $\rho_{dc}(T)$  at a relatively lower temperature region ( $T \leq 10 \text{ K}$ ). The results of the temperature and magnetic field dependences of the MR supported the results of  $\sigma_{dc}$ . As the temperature decreased to 0.7 K, the negative MR unusually increased up to  $\sim 30\%$  compared to zero field resistance.

#### ACKNOWLEDGMENTS

This work was supported by a Korean Research Foundation Grant (KRF-2004-005-C00068) and the SRC (R11-2000-071). The authors thank S. H. Park at Korean Basic Science Institute in Daejeon for assisting measurements of dc conductivity and magnetoresistance.

\*Corresponding author. FAX: +82-2-927-3292; Email address: jjoo@korea.ac.kr

<sup>1</sup>R. Saito, G. Dresselhaus, and M. S. Dresselhaus, *Physical Properties of Carbon Nanotubes* (Imperial College Press, London, 1998).

<sup>2</sup>L. Dai and A. W. H. Mau, *Adv. Mater.* (Weinheim, Ger.) **13**, 899 (2001).

<sup>3</sup>H. M. Kim, K. Kim, C. Y. Lee, J. Joo, S. J. Cho, H. S. Yoon, D. A. Pejaković, J. W. Yoo, and A. J. Epstein, *Appl. Phys. Lett.* **84**, 589 (2004).

<sup>4</sup>S. Barrau, P. Demont, A. Peigney, C. Laurent, and C. Lacabanne, *Macromolecules* **36**, 5187 (2003); L. Valentini, I. Armentano, J. Biagiotti, E. Frulloni, J. M. Kenny, and S. Santucci, *Diamond Relat. Mater.* **12**, 1601 (2003); J. K. W. Sandler, J. E. Kirk, I. A. Kinloch, M. S. P. Shaffer, and A. H. Windle, *Polymer* **44**, 5893 (2003).

<sup>5</sup>B. E. Kilbride, J. N. Coleman, J. Fraysse, P. Fournet, M. Cadek, A. Drury, S. Hutzler, S. Roth, and W. J. Blau, *J. Appl. Phys.* **92**, 4024 (2002).

<sup>6</sup>P. Sheng, E. K. Sichel, and J. I. Gittleman, *Phys. Rev. Lett.* **40**, 1197 (1978).

<sup>7</sup>N. F. Mott and E. A. Davis, *Electronic Processes in Non-crystalline Materials*, 2nd ed. (Clarendon, Oxford, 1979).

<sup>8</sup>K. Hernadi, *Chem. Phys. Lett.* **363**, 169 (2002).

<sup>9</sup>H. M. Kim, K. Kim, S. J. Lee, J. Joo, H. S. Yoon, S. J. Cho, S. C. Lyu, and C. J. Lee, *Curr. Appl. Phys.* **4**, 577 (2004).

<sup>10</sup>D. Stauffer and A. Aharony, *Introduction to Percolation Theory*, 2nd ed. (Taylor & Francis, London, 1992); R. Zallen, *The Physics of Amorphous Solids* (Wiley, New York, 1983).

<sup>11</sup>A. B. Kaiser, G. Düsberg, and S. Roth, *Phys. Rev. B* **57**, 1418 (1998); A. B. Kaiser, G. C. McIntosh, K. Edgar, J. L. Spencer, H. Y. Yu, and Y. W. Park, *Curr. Appl. Phys.* **1**, 50 (2001).

- <sup>12</sup>Y. Yosida and I. Oguro, *J. Appl. Phys.* **83**, 4985 (1998); Y.-H. Lee, D.-H. Kim, H.-Kim, and B.-K. Ju, *ibid.* **88**, 4181 (2000); O. Chauvet, J. M. Benoit, and B. Corraze, *Carbon* **42**, 949 (2004).
- <sup>13</sup>G. T. Kim, E. S. Choi, D. C. Kim, D. S. Suh, Y. W. Park, K. Liu, G. Duesberg, and S. Roth, *Phys. Rev. B* **58**, 16064 (1998); G. C. McIntosh, G. T. Kim, J. G. Park, V. Krstic, M. Burghard, S. H. Jhang, S. W. Lee, S. Roth, and Y. W. Park, *Thin Solid Films* **417**, 67 (2002); A. Fujiwara, K. Tomiyama, H. Suematsu, K. Uchida, and M. Yumura, *Physica B* **298**, 541 (2001).
- <sup>14</sup>H. Fukuyama and K. Yosida, *J. Phys. Soc. Jpn.* **46**, 102 (1979).